# STUDY ON PROCESS OPTIMIZATION AND WETTING PERFORMANCE OF ULTRASONIC-OXIDIZED WOOL FIBER

Ke Li, Wenliang Xue\*, Shen Hua

Key Laboratory of Textile Science & Technology, Donghua University, Ministry of Education, Shanghai, China. \*Corresponding author email: xwl@dhu.edu.cn

### Abstract:

As lightweight and comfortable wool products have become the mainstream of the market, the surface treatment technology of wool fiber has been widely observed. Here, we treated wool fibers by ultrasonic bath and oxidation in a composite method that was better able to improve the wetting properties of wool fiber. Using this approach, we investigated the main factors influencing the effect of treatment and established the regression equations of multiple indices on processing conditions; after testing and optimization, the optimum technological parameters were obtained and experimentally verified. In addition, test results revealed that the ultrasonic-oxidation treatment in the optimum process led to the disulfide bonds (S-S) of wool fiber breaking and being oxidized, but showed less effect on the fiber's supramolecular structure; the wool fiber surface became smoother and more uniform, which resulted in a greatly increased wettability; there was a remarkable decrease in contact angle, and the rate of moisture absorption and desorption was enhanced in response to optimal treatment. These findings are significant for the potential industrial application of wool fiber as a moisture-absorbing material in textile products.

## Keywords:

Wool fiber, surface treatment technology, ultrasonic technology, oxidation, optimization experiment

#### 1. Introduction

A vital raw material for top textiles, wool is a natural keratin fiber with a complex cellular morphology. Since wool fibers have closely arranged cortical cells, they are vulnerable to physical and chemical treatment. The application of physical technology to wool textiles is increasing in the textile industry, such as ultrasonic [1], plasma [2], microwave [3], radiation [4], and so on. Ultrasonic technology has a series of excellent properties and is a high-efficiency technology with low cost and no pollution. Recently, scholars in this field performed considerable research on the use of ultrasonic technology in wool textile products. For instance, Li Q. et al. [5] investigated the changes in fiber structure and chemical behavior via X-ray diffraction (XRD) and Fourier-transform infrared (FTIR) spectroscopy. This showed that ultrasonic treatment rearranged the protein chains in macro fibers into a more regular and less flexible structure. As far as wool fabric is concerned, sustained ultrasonic treatment can lead to significant reduction of fabric strength and elongation. Li Q. et al. [1] reported that ultrasonic scouring was found to improve removal of grease and ash from the wool fibers. It shows that the introduction of ultrasonic devices into traditional wool washing may be a feasible alternative method for the wool scouring industry. Moreover, high-quality dyeing samples can be obtained when ultrasonic technology is applied to wool textile dyeing. Mohammad et al. [6] demonstrated that ultrasound, together with an array of textile auxiliaries,

could prevent dye agglomeration when dyeing wool with acid dyes, which makes wool dyeing even more environmentally friendly than it is now. Ferrero et al. [7] studied the possibility, thanks to the use of ultrasound-assisted treatment, of reducing the dyeing temperature of acid dyes on conventional wool.

The fiber moisture absorption is an important performance indicator that not only affects the fiber performance but also relates to the manufacturing process and comfort of textiles. The improved wetting properties of wool fibers and yarns allow fabric to be cooler and less damp in hot and humid conditions. As the fiber material can adjust the micro-environment inside the garment by absorbing and dispersing moisture, it can adapt to the ambient temperature and humidity [8]. Recent research shows that a mixed hydration model overseen by a scanning electronic microscope (SME) mechanism will be produced after wool fibers absorb water [9,10]. The moisture absorption performance of wool fiber hinges on its chemical composition and fiber structure. The scale layer of wool fiber is mainly composed of lipids (25%) and protein (75%), and the most abundant amino acid in the protein is cystine [11,12]. The scales of wool fibers have water repellency, but they are arranged in annular or tile-like coatings, the scale surface overlaps between scales are small, and there are gaps at the junction. The porosity between scales has friction and hindrance to water molecules, which is beneficial to water absorption and retention. At the same time, the cortex of wool fiber contains more hydrophilic groups (such as -OH, -COOH,

and -CONH<sub>2</sub>), which gives wool potential strong moisture absorption ability. Textile researchers have always changed the surface structure of wool fibers by scaling modification [13]: as an example, the commonly used oxidation method of wool surface treatment technology can reduce the lipids in wool fiber scales and rise the number of hydrophilic groups [14]. With the increase of scale peeling degree, the hydrophilicity of fibers was markedly improved. In addition, differential scanning calorimetry (DSC) analysis showed that the water absorption capacity of wool fiber surface could also be enhanced by proper ultrasonic treatment [15], but the related research is still rarely reported.

In this article, we describe how wool fiber was treated by the oxidation method in an ultrasonic bath. We optimized the parameter combinations via orthogonal test to determine the main factors influencing the ultrasonic-assisted oxidation treatment of wool fibers and used the quadratic orthogonal rotary combination design method to establish the regression equations of multiple indices on processing conditions [16]. Then, we determined optimal treatment conditions by the Objective Programming method according to various comprehensive indices of multiple experiments, which made wool fibers achieve superior surface scaling effects on the basis of good tensile properties. Furthermore, the molecular structure, surface morphology, and wetting properties of wool samples treated by the optimal process were studied, which provided a reference for the wool fiber surface treatment technology in the ultrasound process.

#### 2. Experimental

## 2.1. Materials

Wool yarns used in this study were obtained from Jiangsu Lugang Science and Technology Co., Ltd. (Jiang Su, China); nano-calcium carbonate was purchased from Shanghai Chenqi Chemical Engineering Science and Technology Co., Ltd. (Shanghai, China); sodium hydrogen sulfite was purchased from Wei Zhenyuan Medical Science and Technology Co., Ltd. (Fujian, China); hydrochloric acid was purchased from Bo Linda Science and Technology Co., Ltd. (Shenzhen, China); ethanol was purchased from Rui Kang Medical Science and Technology Co., Ltd. (Hebei, China). All chemicals used in wool treatment were of analytical grade, unless otherwise stated.

# 2.2. Sample treatment methods

The ultrasonic machine JAC-4020P (KODO Washing Machine Company, South Korea) was operated at 50 kHz with effective power of 400 W and heating power of 500 W. Wool fiber can be oxidized in a variety of ways, and the method used in this paper is chlorination. The original wool yarns were inserted in a conical flask containing sodium hypochlorite and hydrochloric acid and immersed in an ultrasonic bath. Nano-calcium carbonate was dissolved in ethanol to prepare an alkaline solution, which can help neutralize solution pH. The ultrasonic machine was kept consistently warm during the experiment process of ultrasonication.

#### 2.3. Analysis and measurement

Variations in the chemical structure of wool fiber were investigated on a Nicolet 6700 FTIR spectrometer (Thermo Fisher, United States), and the wave number range used was 500-4000 cm<sup>-1</sup>. The surface morphology of wool fiber samples was observed with a FlexSEM1000 (Hitachi Ltd., Japan). To analyze the tensile properties of the wool yarn samples, the YG021E Single Yarn Strength Tester (Jiangsu, China) was used to measure the elongation at break and breaking strength of yarns with a clamping speed of 500 mm/min and a pre-tension of 10 cN. To determine the wetting property of wool fabrics, the contact angles were measured by the air bubble method using a OCA15EC optical contact angle meter (Dataphysics, Germany).

Moisture absorption test: The wool yarn sample of about 1g was dried in an oven to gain the dry weight, quickly taken out and moved to the standard atmosphere (temperature of 20  $\pm$  2°C and relative humidity of 65%  $\pm$  3%), weighted as the initial weight, then the quality of sample was recorded every 5 minutes until the fiber reached the moisture absorption balance.

Moisture desorption test: The specimen of 1g wool yarn was placed in a moisture-determining instrument at relative humidity (95  $\pm$  5%) to reach the saturation state; then was moved to the standard atmospheric condition immediately and the initial weight recorded; this was recorded several more times at 5-minute intervals until the fiber reached the moisture desorption balance. We then dried the sample to gain the dry weight. The percent moisture content Mt is defined as:

$$M_{t} = \frac{W_{t} - W_{i}}{W_{i}} \times 100\% \tag{1}$$

where  $W_{t}$  is the weight of moist material and  $W_{i}$  is the weight of dry material.

Scaling index studies were used to assess the removal effect on a wool fiber scale. Each treated wool sample was observed by SEM images of 100 wool fibers. According to Figure 1, the scale removal degree was gained to the following three degrees: low, medium, and high. The scale borders of wool fiber are visible in a high-scale state (Figure 1a); the outline scale of medium-scale wool became blurry, the thickness became thinner close to the hair stem as well, and the density became significantly less (Figure 3b). The scales of low scaly wool fiber nearly disappeared completely, leaving only the hair stem (Figure 3c). The scaling index was calculated according to the following formula:

Scaling index = 
$$\frac{(R_M + R_H) \times 10}{R}$$
 (2)

Where  $\rm R_{_{\rm M}}$  and  $\rm R_{_{\rm H}}$  is the number of medium-scale and high-scale wool fiber, respectively; R is the total number of all wool fiber.

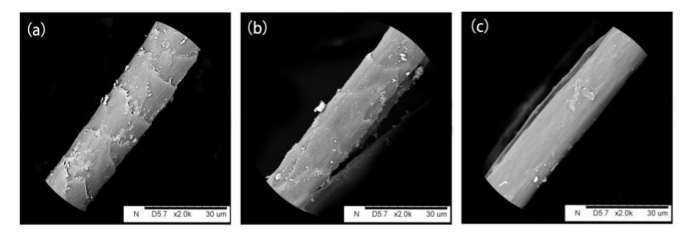


**Figure 1.** The surface state of the wool fiber samples. (a) high-scale wool fiber; (b) medium-scale wool fiber; (c) low-scale wool fiber.

#### 3. Results and discussion

#### 3.1. Orthogonal test

The orthogonal experiment of four factors at three different levels was carried out, as shown in Table 1. Reaction time of HCI and NaCIO, treatment time of nano-size CaCO<sub>3</sub>, and temperature and concentration of NaCIO are the key process parameters in the experiment. Tensile strength, breaking elongation of yarn, and scaling index were selected as the evaluation indexes in this experiment. Tensile strength and elongation at break of yarn are two important physical measures to characterize the mechanical properties of yarn

or fabric. Observe the change of scales of samples 1-9 in each sample: the larger the scaling index is, the more scales were removed. Experiments were conducted according to the orthogonal design table, and the simulation results are shown in Table 2. Table 3 illustrates the effects of four processing parameters on the experimental index through range analysis. It follows that it is difficult to obtain an optimal technical parameter that combined every property. Therefore, the processing parameters need to be compromised in terms of the specific requirements. In addition, the results of variance analysis [16] are as follows, according to Table 3.

We derived from this that treatment results are mainly affected by factor A (reaction time of HCl and NaClO) and factor B (treatment time of nano-size  ${\rm CaCO_{3)}}$  within the set range of factors.

### 3.2. Quadratic regression general rotation design

Based on the results of the orthogonal test, the reaction time of HCl and NaClO and the treatment time of nano-size CaCO<sub>3</sub> were taken as the optimized parameters. In order to use the Quadratic Regression General Rotation Design (QRGRD), the

Table 1. The orthogonal test table

	Factor									
Level	Reaction Time of HCI and NaCIO (min)(A)	Treatment Time of N"ano-size CaCO <sub>3</sub> (min) (B)	Reaction Temperature (°C) (C)	Concentration of NaCIO (ml) (D)						
1	0	25	40	10						
2	20	35	45	15						
3	40	45	50	20						

Table 2. The results of range analysis and variance analysis

Factor Number		Fac	ctor		Experiment indices				
	Α	В	С	D	Tensile strength (cN/Tex)	Breaking elongation (%)	Scaling Index		
1	1	1	1	1	0.48	9.69	4.8		
2	1	2	2	2	0.67	6.89	4.2		
3	1	3	3	3	0.92	8.91	5.4		
4	2	1	2	3	0.24	3.28	5.5		
5	2	2	3	1	0.32	4.96	6.2		
6	2	3	1	2	0.67	6.59	7.6		
7	3	1	3	2	0.43	4.66	5.5		
8	3	2	1	3	0.38	5.16	6.22		
9	3	3	2	1	0.82	9.52	6.78		

http://www.autexrj.com/

Table 3. The results of range analysis and variance analysis

Fuel vetien Index		Range a	analysis		Variance analysis				
Evaluation Index	R <sub>A</sub>	R <sub>B</sub>	R <sub>c</sub>	R <sub>D</sub>	F <sub>A</sub>	F <sub>B</sub>	F <sub>c</sub>	F <sub>D</sub>	
Tensile strength	0.280	0.420	0.067	0.077	16.857	43.143	1.000	1.286	
	The orde	er of influentia	I factors: B→	A→D→C	F <sub>0.1</sub> =9, F <sub>0.05</sub> =19, F <sub>0.01</sub> =99				
Dungling algorithm	3.553	2.670	0.970	2.273	13.340	9.252	1.000	6.483	
Breaking elongation	The orde	er of influentia	l factors: A→l	B→D→C	F <sub>0.1</sub> =9, F <sub>0.05</sub> =19, F <sub>0.01</sub> =99				
Onalia a in day	1.727	0.764	0.634	0.257	73.194	46.387	11.774	1.000	
Scaling index	The order of influential factors: $A \rightarrow B \rightarrow C \rightarrow D$ $F_{0.1} = 9, F_{0.05} = 19, F_{0.01} = 99$								

Table 4. Natural factors level code table of two factors.

	Factor						
Level	Reaction Time of HCl and NaClO (min) (x <sub>1</sub> )	Treatment Time of Nano-size CaCO <sub>3</sub> (min) (x <sub>2</sub> )					
+r (+1.414)	40	45					
1	34.14	42.07					
0	20	35					
-1	5.86	27.93					
-r (-1.414)	0	25					
Δj	14.144	7.072					

ranges of the two parameters should be estimated first. Through the orthogonal experimental design above, the reaction time of HCl and NaClO ranges was specified as 0–40 min, and the treatment time of the nano-size  ${\rm CaCO_3}$  range was 25–45 min. The natural factors level code table of two factors is shown in Table 4. Here,  ${\rm x_i}$  is the coded formula and the two factors were divided into five levels: those codes are +r, 1, 0, -1 and -r. Based on the aforementioned natural factors level code table of the QGRUD method, 13 samples with various processing parameters were designed via the quadratic general rotary unitized design method. The detailed parameters and the results of the experiment are shown in Table 5.

The regression equation was established via the QRGRD method. In order to determine the authenticity and reliability of Eq, F-test was applied to both the simulant test and the regression equation test, the regression coefficients were tested by the T-test method. The quadratic regression equations obtained in terms of coded value after neglecting nonsignificant coefficients are given as:

$$y_1^{\ \ \ } = 0.33 + 0.1521 \, x_2^{\ \ \ } + 0.1412 \, x_1^{\ \ 2} + 0.1063 x_2^{\ \ 2}$$

$$y_2^{\Lambda} = 4.25 + 1.1704 x_2 - 1.4029 x_1 x_2 + 1.8794 x_1^2$$
  
 $y_3^{\Lambda} = 12.99 + 0.9612 x_1 - 0.1521 x_2 - 1.9926 x_1^2 - 0.6863 x_2^2$ 

where x1 and x2 respectively represent the coding space values of the reaction time of HCl and NaClO, and the treatment time of nano-size CaCO3, y1 and y2 indicate tensile strength and breaking elongation, respectively.

The 3D response surface and 2D contour plot are the graphical representations of the regression equation, which were utilized to study the effect of each variable on the processing results. In Figure 2, the response surfaces of three indexes were plotted versus reaction time of HCl and NaClO, and treatment time of nano-size CaCO<sub>3</sub> variables, while the remaining variables were kept at zero level. When the reaction time of the CaCO, ultrasonic bath is held constant, increasing the reaction time of HCl and NaClO caused the descaling degree to first grow and then decrease, and the break elongation and tensile strength to decline initially and subsequently improve. This is because, in the initial stage of the experiment, the longer the reaction time of HCl and NaClO, the more Cl<sub>2</sub> is produced, and the scale of wool fiber is removed in the ultrasonic bath, which affects the elasticity and strength loss of the yarn. As the reaction proceeded, Cl<sub>2</sub> was partly lost after the complete reaction of HCl and NaClO. The oxidation reaction on the surface of wool fiber could not be carried out because the solution was not immersed in the ultrasonic bath in time. When the reaction time of HCl and NaClO is fixed, with the extension of the reaction time of CaCO<sub>3</sub>, the scale peeling degree went up first and then showed a downward trend, and the break strength became lower first and then gradually recovered. When the reaction of HCI and NaCIO can only produce a small amount of Cl<sub>2</sub>, the wool fiber is mainly affected by ultrasonic waves in the CaCO<sub>3</sub> bath, there has been a steady rise in the yarn break elongation; further, when the treatment reached a sufficient amount of Cl<sub>2</sub>, the oxidation of wool fiber in the ultrasonic bath triggered elastic damage, causing the elongation at break of wool yarn to fall slightly.

 Table 5. Quadratic regression general rotation design and results.

Run	X <sub>0</sub>	<b>X</b> <sub>1</sub>	X <sub>2</sub>	X <sub>1</sub> x <sub>2</sub>	X <sub>1</sub> <sup>2</sup>	X <sub>2</sub> <sup>2</sup>	Tensile strength (cN/Tex)	Breaking elongation (%)	Scaling Index
1	1	1	1	1	1	1	0.92	8.91	6.46
2	1	1	-1	-1	1	1	0.48	9.69	4.81
3	1	-1	-1	-1	1	1	0.40	9.67	4.65
4	1	-1	1	1	1	1	0.86	9.52	6.78
5	1	1.414	0	0	2	0	0.38	5.16	6.22
6	1	-1.414	0	0	2	0	0.67	6.89	4.23
7	1	0	1.414	0	0	2	0.67	6.59	7.59
8	1	0	-1.414	0	0	2	0.24	3.28	5.56
9	1	0	0	0	0	0	0.32	4.96	6.23
10	1	0	0	0	0	0	0.36	4.65	5.98
11	1	0	0	0	0	0	0.38	4.23	6.15
12	1	0	0	0	0	0	0.29	3.43	6.25
13	1	0	0	0	0	0	0.30	3.98	6.08

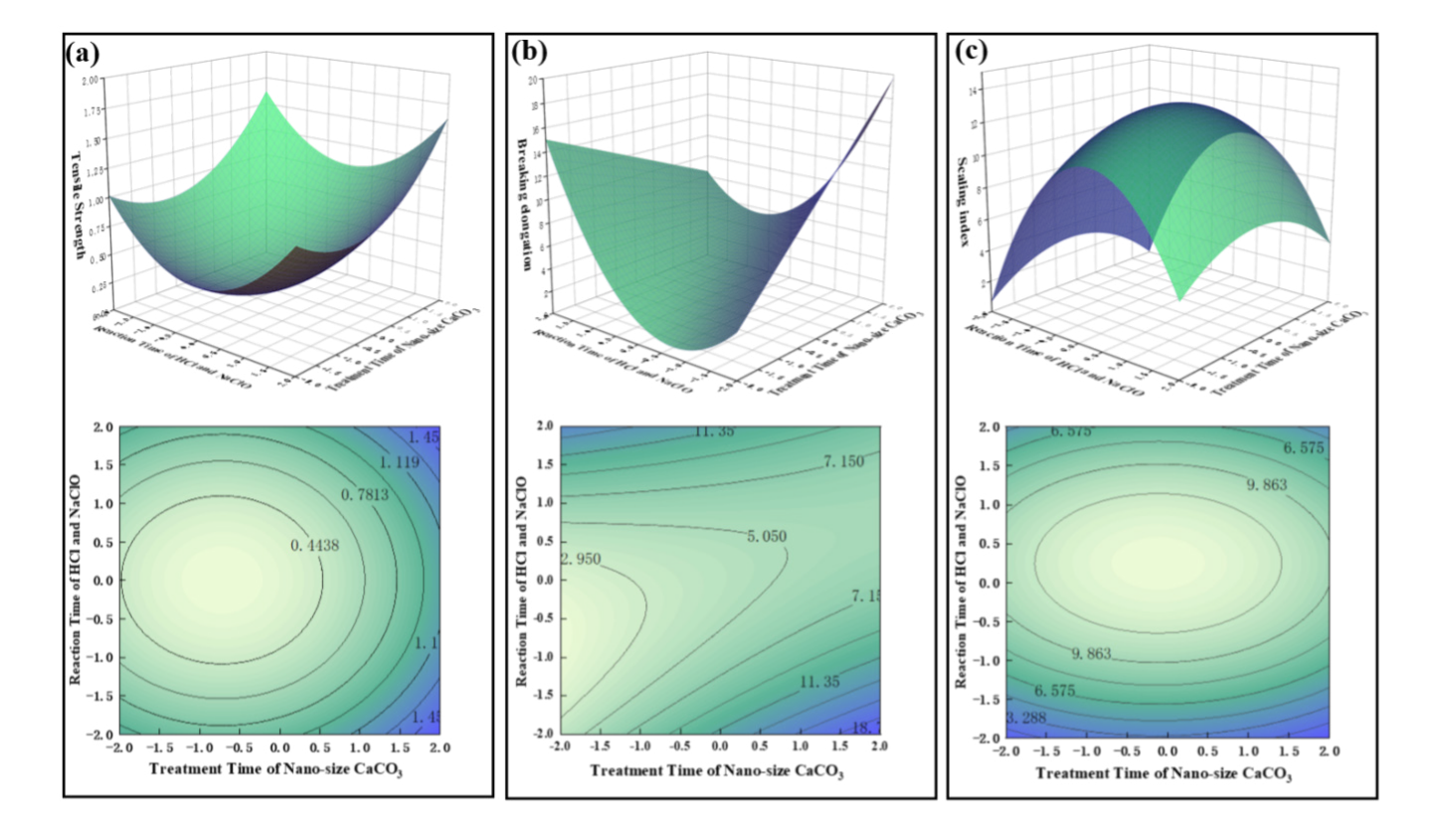


Figure 2. Effects of the reaction time of HCl and NaClO, and reaction time of HCl and NaClO on wool samples. (a) Tensile strength (b) Breaking elongation (c) Scaling index.

Through the high-precision and effective regression equation between the test factors and the investigation indexes obtained by the optimal test design, the optimization mathematical model can be established by the Objective Programming method. The objective function can be constructed as follows:

$$\min F(x), x \in R_n \tag{3}$$

s. t. 
$$\{g_u(x), u = 1, 2, 3, 4\}$$
 (4)

$$F(X) = [F_1(X)/f_1^{(0)} - 1]^2 + [F_2(X)/f_2^{(0)} - 1]^2 + [F_3(X)/f_3^{(0)} - 1]^2$$
 (5)

Where  $F_1(x)=y_{Tensile\ strength}$ ,  $F_2(x)=y_{Breaking\ Elongation}$ ,  $F_3(x)=y_{Scaling\ degree}$ .  $f_i(0)$  is the ideal optimal value of the corresponding index in the experimental range, the values were selected as: breaking strength of 0.92 cN/Tex, breaking elongation of 9.69%, and scaling index of 7.59, respectively. The parameters are optimized under the following constraints:

s.t. { 
$$g_1 = 1.414 + x_1 \ge 0, g_2 = 1.414 - x_1 \ge 0$$
 (6)  $g_3 = 1.414 + x_2 \ge 0, g_4 = 1.414 - x_2 \ge 0$ 

The optimal parameter combination was observed based on the condition that the four objective functions were simultaneously close to each other. The optimized results after decoding were given as follows: the reaction time of HCl and NaClO was 32 min, the treatment time of nano-size  $\text{CaCO}_3$  was 42 min. To verify the accuracy of the results of the optimization analysis, the optimum parameters were chosen under the same experimental conditions for three repeated verification tests. The validation test results show that the optimization results are reliable, which are: breaking strength of 0.85 cN/ Tex, breaking elongation of 9.23%, and scaling index of 7.02, respectively.

## 3.3. Properties of optimal wool sample

## 3.3.1. FTIR spectroscopy

Figure 3a depicts the infrared spectrum of raw and treated wool fiber, from 4000 to 500cm<sup>-1</sup> in the FTIR spectra. As can be seen from Figure 3b, the disulfide bond of cystine will produce corresponding intermediate products according to different oxidation pathways, and the final oxidation product is sulfoalanine. Figure 3c presents the FTIR spectroscopy in the range of 1300-1000 cm<sup>-1</sup> (sulfur oxygen vibration zone), there is a clear trend of increasing the intensity of absorption vibration peaks at 1079 cm<sup>-1</sup> and 1043 cm<sup>-1</sup>. The infrared absorption peaks were mainly assigned to the symmetric stretching vibration of S—O in SO3— and SSO3— at 1079 cm<sup>-1</sup> and 1043 cm<sup>-1</sup>, respectively. This is due to the amorphous region producing energy concentration when ultrasonic waves affect wool fiber, making the crack extend and the specific surface area increase, which will lead to microslip on the fiber surface and fatigue cracks. A comparison of the two samples reveals that ultrasonic oxidation treatment broke the disulfide bonds (S-S) and generated final oxidation products that destroyed the scale layer on the wool fiber surface. In addition, it can be seen from Figure 3d that the treated wool fiber showed obvious characteristic absorption peaks at 1744cm<sup>-1</sup> (C=O), and the intensity of the absorption peak at 1261cm<sup>-1</sup>( $\delta$ —OH) decreased slightly, compared with the sample of original wool. This is mainly due to the oxidation of a number of hydroxyl groups to carbonyl groups.

As shown in Figure 3d, the spectrum of wool fibers in the infrared range has a number of characteristic bands containing secondary structure-related information of transformations from alpha to beta conformation. The vibration absorption peaks were mainly assigned to C=O and the bending vibration of C-N—H in CONH—— at 1700–1640 cm<sup>-1</sup> (amide I) and 1530–1510 cm<sup>-1</sup>(amide II), respectively. The 1300–1240 cm<sup>-1</sup> component has been attributed to  $\alpha$ -helical conformation and segments of disordered structure. The corresponding infrared spectrum of β-pleated sheet conformation appears from 1240 to 1230 cm<sup>-1</sup>. A detailed FTIR graph shows that no significant change between the two samples was evident, but that treated wool fibers have an increased number of waves corresponding to the infrared peaks than the untreated samples. This is due to the single ultrasonic treatment weakening the hydrogen bonding between wool molecules and increasing the gap in the amorphous region; this cannot change the supramolecular structure of wool fibers [11]. The oxidation-ultrasonic treatment not only leads to changes in the intermolecular forces of wool fibers, but also affects their supramolecular structure, which is important for the mechanical structure and wetting properties of wool fiber and yarn.

#### 3.3.2. The surface morphology

SEM images of wool samples before and after optimized treatment are given in Figure 4. The scales of untreated wool fiber were annularly located, each of which formed a ring around the hair stem, and the root of one scale was covered by the tip of the other scale, as shown in Figure 4a. The scales were densely covered, and the thickness were not uniform, with uneven and wavy edges. The border of some scales on the treated wool fiber became blunt, and the thickness changed slightly, as shown in Figure 2b. The scale surface was smoother and more regular, with a few fragments of broken scales. This is due to the fact that the disulfide bond of cystine was oxidized to absorbent groups, such as the sulfonic acid group, during the treatment. The cuticle on the outer surface of the wool fiber swelled, softened, and lost weight, the impaired portion became a compound that can be dissolved in solution. Thus, the wool scale layers were partly stripped off, which has a considerable impact on the wettability of the wool.

## 3.3.3. Wetting properties

Table 6 shows one of the test results of the contact angle on raw and optimal treated wool samples. It can be seen that the contact angle of the treated sample was lowered markedly relative to that of the raw wool sample. According to the airbubble approach, the trapped bubbles will adhere; this is similar to the adsorption of liquid on solid surfaces in air, when they contact the solid surface of the glass slide wrapped with yarn. Changes on the cuticle layer of treated wool engender hydrophilic group increases and lipid decreases in number on

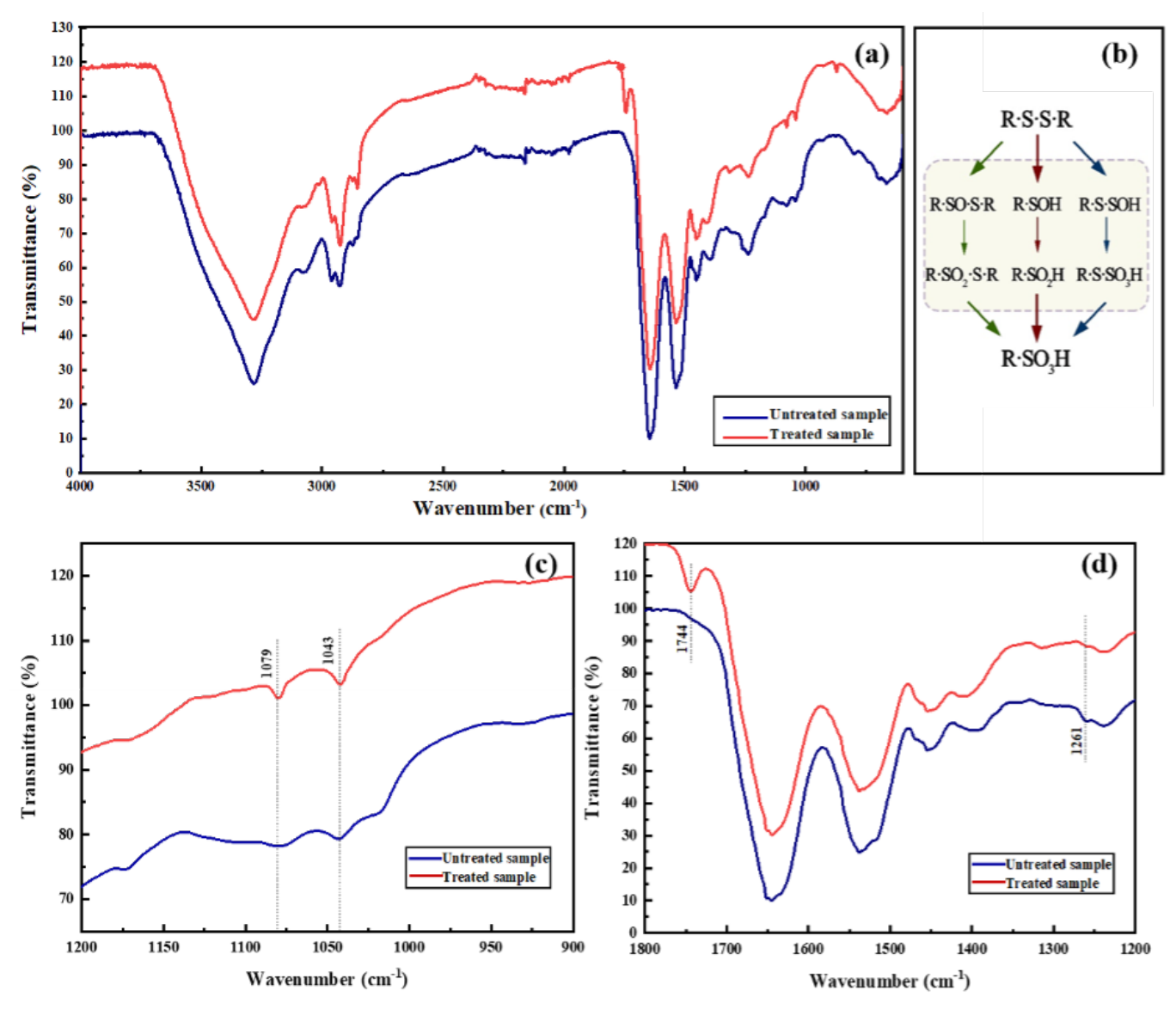
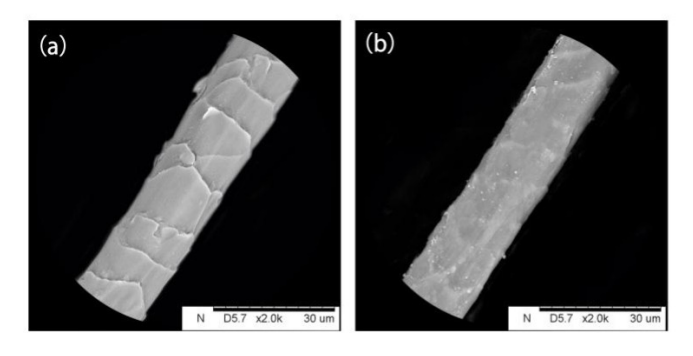


Figure 3. FTIR spectroscopy of untreated and treated wool samples. (a) FTIR in the range of 4000–600 (b) the oxidation process of cystine disulfide bond (c) FTIR in the range of 1200–900 (d) FTIR in the range of 1800–1200.



**Figure 4.** The surface morphology of wool fiber. (a) untreated wool fiber (b) treated wool fiber.

the fiber surface, contributing to improved hydrophilicity of wool fiber [16]. The results reveal that the wettability of oxidized-ultrasonic wool yarn was significantly raised with fiber, leading to the angle reduction between the liquid and the sample-gas interface.

The regression curves of moisture absorption and liberation equation were obtained via the curve fitting method in line with the experimental data, as shown in Figure 5a. It can be seen that the moisture absorption curve of wool fiber before and after oxidized-ultrasonic treatment are basically the same. In the initial stage, the moisture regains of both samples were dramatically increased, with fast moisture absorption rate; then after about 50 minutes, the rate began to slow down, and the curve steadied until absorption equilibrium was reached. Figure 4b reveals that there were similar moisture desorption curves of raw and optimally treated wool fibers, and both of them feature a fast and then slow moisture desorption rate. As can be seen in Figure 5c and 5d, the regression curves of moisture absorption and liberation rate equilibrium of raw and treated wool fibers are exponential functions, on the basis of the equation for regression curves of moisture absorption and liberation rate[9]. In the whole moisture absorption and desorption process, the moisture regain of the treated wool sample was evidently higher than that of the ordinary wool fiber, which can be ascribed to the improvement of the wettability of the wool fiber surface. The major cause is that

http://www.autexrj.com/

Table 6. Contact Angle of wool samples

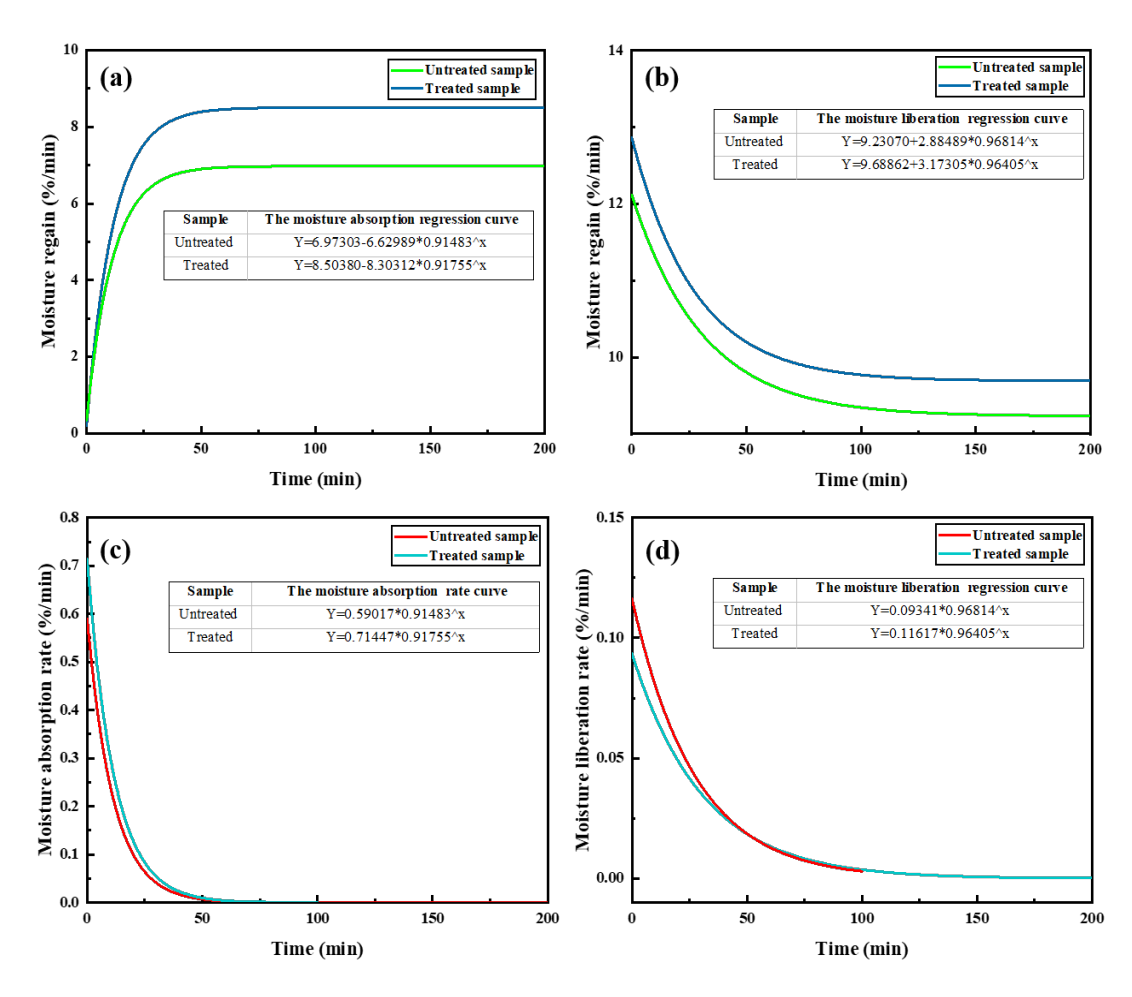
		Untreated sample	Treated sample		
Contact Angle	Clase PLT/ Chapte IT-37		Challet 787		
	Left	89.7°	Left	28.0°	
	Right	89.5°	Right	27.8°	

the moisture regain of wool fiber improves with the degree of scale peeling [8]. The modification on the wool cuticle layer can relatively enhance hydrophilicity and water capacity potential, as a consequence of reduction in cystine content and gain in hydrophilic groups. Besides, in contrast to raw wool, optimally treated wool yarn required more time to reach the moisture absorption and desorption equilibrium. This is because the raw wool fiber surface has high hydrophobicity owing to the large amount of lipoid, and it mainly absorbs water indirectly, due to the weak force of the bond between water molecules and fibers. The protein structure of the treated wool fiber surface

is altered and the lipoid decreased. The fiber mainly absorbed water by hydrophilic groups with stronger binding force, leading to a longer equilibrium time for wool yarn.

#### 4. CONCLUSIONS

In this article, wool fiber scale was oxidized with the assistance of an ultrasonic bath, and the factors affecting the treatment effect of wool fiber were derived by designing orthogonal experiments. On this basis, the regression equation under



Figure

multivariate indexes was established by quadratic orthogonal rotational combination design, and the parameters were optimized as: the reaction time of HCl and NaClO was 32min, the treatment time of nano-size CaCO<sub>3</sub> was 42min, respectively. The optimization results are relatively reliable according to the experimental values under the same conditions. In addition, the ultrasonic-oxidation treatment caused the disulfide bonds (S-S) of wool fibers to break and be oxidized, but showed less effect on the fiber supramolecular structure. The wool fiber surface became smoother and more uniform due to scale reduction and shedding, which resulted in a significant increase of wettability and accelerated the rate of moisture absorption and desorption. The treated woolen yarn with excellent moisture absorption can be used in lightweight wool fabrics with high-grade quality to improve apparel comfort, or further in the development of smart wool textile products as a natural wet-driven material.

# Acknowledgement

This work was supported by the [the Fundamental Research Funds for the Central Universities] under Grant [2232022G-01].

#### References

- [1] Li, Q., et al. (2014). Adapting ultrasonic assisted wool scouring for industrial application. Textile Research Journal, 84(11), 1183-1190.
- [2] Rahul, N., et al. (2018). Influence of dielectric barrier discharge treatment on mechanical and dyeing properties of wool. Plasma Science and Technology, 20(6).
- [3] Mowafi, et al. (2014). Microwave-Assisted Bleaching of Wool Fabrics. Journal of Natural Fiber, 12 (2), 97-107.
- [4] Xin, J. H., et al. (2006). Surface modification and low temperature dyeing properties of wool treated by UV radiation. Coloration Technology, 118(4), 169-173.

- [5] Qing, L., et al. (2012). Effects of ultrasonic treatment on wool fiber and fabric properties. The Journal of The Textile Institute, 103(6), 662-668.
- [6] Mohammad, M. H., et al. (2017). Ultrasound-Assisted Ultralow Liquor Ratio Dyeing of Wool Textiles with an Acid Dye. ACS Sustainable Chemistry & Engineering, 5 (1), 973-981.
- [7] Ferrero, F., et al. (2017). Ultrasound for low temperature dyeing of wool with acid dye. Ultrasonics Sonochemistry, 19(3), 601-606.
- [8] Wong, L. (2017). Moisture Absorption and Perspiration Performance of Wool Fiber Scale Layer on Wool Shirts Impact. Wool Technology, 45 (12), 73–75.
- [9] Lin, X., et al. (2012). Moisture absorption properties of wool with different fineness Research. Wool technology, 41 (10), 49-52.
- [10] Hu, J. L., et al. (2020). Wool can be cool: Water-actuating woolen knitwear for both hot and cold. Advanced Functional Materials, 30(51).
- [11] Xiao, X. L., et al. (2017). Mechanism study of biopolymer hair as a coupled thermo-water responsive smart material. Smart Materials and Structures, 26 (3), 035023.
- [12] Pelton, J. T., et al. (2000). Spectroscopic methods for analysis of protein secondary structure. Analytical Biochemistry, 277 (2), 167-176.
- [13] Zhang, H., et al., (2013). The effect of wool surface and interior modification on subsequent photostability. Journal of Applied Polymer Science, 127(5), 3435-3440.
- [14] Yu, X.W., et al. (2005). A biological treatment technique for wool textile. Brazilian Archives of Biology and Technology, 48(5), 675-680.
- [15] Li, G., et al. (2017). Effect of ultrasonic treatment on the thermal and mechanical properties of wool fabrics. Wool Textile Journal, 45(8), 48-51.
- [16] Ca,i Z. Y., Wang, Z. X. (1985). The application of orthogonal design in concrete. China Building Industry Press (China).

http://www.autexrj.com/